STRUCTURE OF COMMERCIAL IRON CATALYST UNDER AMMONIA DECOMPOSITION

Part 1: Determination of Phases Appeared and Their Lattice Parameters

By

Toshiji MATSUI and Isamu TOYOSHIMA*)

(Received Aug. 1, 1962)

Abstract

Constituent phases and their lattice parameters have been determined by x-ray and electron diffraction with catalysts at three typical points on hysteresis loop of rate of steady decomposition of ammonia, revealed by decreasing and then increasing constant hydrogen inflow rate N_H stepwise at fixed inflow rate N_A of ammonia over doubly promoted iron catalyst kept at constant temperature around 450°C.

Catalyst at point $N_H/N_A=0$ consisted solely of γ'-phase except just at the inlet of the catalyst bed, where a small amount of ε-phase coexisted with the main γ'-phase and that at point $N_H/N_A=1$ on the upper curve of the loop observed on decreasing N_H was similarly composed solely of α-phase except at the inlet of the bed, where a small amount of γ'-phase coexisted with the main α-phase. Catalyst at point $N_H/N_A=1$ on the lower curve of the loop observed on increasing N_H, on the other hand, was composed solely of γ'-phase or α-phase at the inlet or outlet of the bed, both the phases coexisting at the middle. Nitrogen content at least in case of the catalyst at point $N_H/N_A=0$ was concluded from the observation of lattice parameter and coexistent phases to decrease along the line of flow in the catalyst bed.

These compositions of the catalysts are in good agreement with those concluded by TOYOSHIMA and HORIUTI from the kinetic analysis of the hysteresis loop on the basis of the mechanism of ammonia decomposition advanced by them.

Electron micrographs of surfaces of the catalysts exhibited "pore" and "crack" structures similar to those observed by MCCARTNEY *et al.* with fused iron catalyst and indicated that the pore is nothing but intergranular void. Surface features of iron single crystals inserted in the bed were much different from those of the catalyst with respect to the "pore" structure, from which the promoter comprized in the catalyst was concluded to be inhibiting surface migration of iron atoms.

*) T. M. and I. T.; Research Institute for Catalysis, Hokkaido University.

Introduction

TOYOSHIMA and HORIUTI[1] recently observed the rate of steady decomposition of ammonia allowing mixture of ammonia and hydrogen to flow at constant rate over doubly promoted iron catalyst at constant total pressure and constant temperature around 450°C. They found thus a stable and reproducible hysteresis of the rate of the steady decomposition by stepwise decreasing and then similarly increasing the constant inflow rate of hydrogen at a fixed inflow rate of ammonia; the steady decomposition rate was higher on stepwise decreasing the inflow rate of hydrogen than that observed on the similar increase over a certain range of hydrogen inflow rate. This result of observation was shown satisfactorily accounted for on the basis of their mechanism of ammonia decomposition[2] with reference to the known equilibrium of iron-nitrogen system[3] but not of the usually accepted mechanism[4], which attributes the rate-determining step to the recombination of adsorbed nitrogen atoms.

It follows from the explanation[1] of the hysteresis that the catalyst's surface is in the state either of α- or γ'-phase at the same constant inflow rate of hydrogen according as the latter is in course of stepwise decrease or increase over a certain range, resulting respectively in the higher or lower curve of the hysteresis. The present paper is concerned with investigation of the above conclusion by x-ray and electron diffraction. The surface of the catalyst was investigated besides by electron microscopy in comparison with that of iron single crystal inserted in the catalyst bed for information as to the effect of promoter comprized in the catalyst.

The catalyst used in the present work is a different portion of the same batch of preparation as that used for the determination[5] of the stoichiometric number of the rate-determining step of the catalyzed synthesis of ammonia.

Experimental

§ 1. Hysteresis

We might briefly sketch the general features of the hysteresis loop which lead to the present procedures of experiment described in subsequent sections. The rate of steady decomposition attained at constant inflow rate of ammonia N_A, that of hydrogen N_H, constant total pressure and constant temperature is expressed by $R \equiv 100\ (N_A - N'_A)/N_A$, *i. e.* the percent of ammonia steadily decomposed, where N'_A is the steady outflow rate of ammonia. Fig. 1 (a) shows the plot of R against N_H/N_A at 487°C and 1 atm. total pressure, where N_A was fixed at 70.0 cc NTP min^{-1} and the constant value of N_H/N_A was stepwise

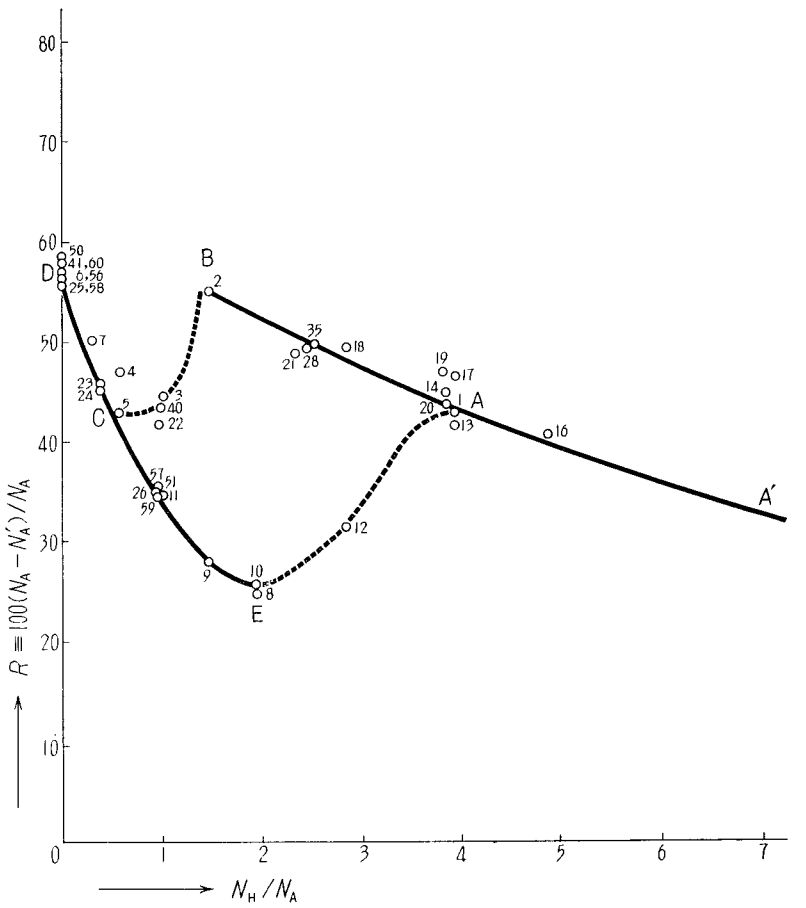

Fig. 1 (a). Hysteresis of percent R of ammonia decomposition. 487°C, $N_A = 70$ cc NTP min^{-1}.

decreased from 10 down to zero, at each of which a steady value of N'_A and hence R were attained, and then similarly increased. R increases monotonously with decrease of N_H/N_A along the curve A'AB up to B, where $N_H/N_A = 1.5$, then steeply decreases down to C and increases again up to D, where $N_H = 0$. Increasing now the constant value of N_H/N_A stepwise, R decreases just following the former curve reversely down to C, but from there on runs lower to decrease down to E and then increases to join the former curve A'AB around $N_H/N_A = 4$, where the reaction $4Fe + NH_3 = Fe_4N + 3/2\ H_2$ is in equilibrium, thus completing the hysteresis. The catalyst was examined at three typical points on such a hysteresis loop, *i. e.* (I) that at the point $N_H/N_A = 0$, (II) that on the lower curve of the hysteresis loop and (III) that on

TABLE 1 (a). Hysteresis of ammonia decomposition*)

Inflow rate N_A of NH_3: 3.125×10^{-3} mol min^{-1} = 70.0 cc NTPmin^{-1}

No. of runs	Temperature**) (°C)					Inflow rate N_H of H_2 mol $min^{-1}\times10_3$	$\frac{N_H}{N_A}$	Outflow rate N_A of NH_3 mol $min^{-1}\times10^3$	Percent decomposition of NH_3 $R\equiv100\,\frac{N_A-N'_A}{N_A}$
	t_1	t_2	t_3	t^4	ave.				
1	484	448	484	496	487	12.41	3.97	1.793	42.6
2	484	484	484	496	487	4.656	1.49	1.414	54.8
3	484	484	486	496	488	3.156	1.01	1.745	44.2
4	484	484	486	496	488	1.788	0.57	1.659	46.9
5	484	484	481	496	486	1.788	0.57	1.794	42.6
6	484	484	481	496	486	0	0	1.370	56.2
7	484	484	481	496	486	0.981	0.31	1.563	50.0
8	484	484	486	496	488	6.125	1.96	2.344	25.0
9	484	484	486	496	488	4.656	1.49	2.257	27.8
10	484	484	484	496	487	6.125	1.96	2.331	25.4
11	484	484	484	496	487	3.156	1.01	2.047	34.5
12	484	484	484	496	487	2.149	2.86	2.149	31.2
13	484	484	484	496	487	12.41	3.97	1.817	41.9
14	484	484	484	446	487	11.97	8.83	1.676	46.6
15	484	481	486	501	488	28.75	9.92	2.500	20.0
16	484	484	484	496	487	15.23	4.89	1.363	40.4
17	484	484	484	496	487	12.41	3.97	1.680	46.3
18	484	484	484	496	487	8.938	2.86	1.580	49.4
19	484	484	484	496	487	11.97	3.83	1.661	46.9
20	484	481	481	496	487	12.13	3.88	1.766	43.5

21	484	484	481	496	487	7.500	2.40	1.603	48.6
22	486	484	481	496	487	3.056	0.98	1.828	41.5
23	486	484	481	496	487	1.228	0.39	1.702	45.6
24	486	484	481	496	487	1.228	0.39	1.717	41.5
25	486	484	481	496	487	0	0	1.387	55.6
26	486	484	484	496	487	3.056	0.98	2.037	34.8
27	486	484	481	496	487	12.14	3.88	1.725	44.8
28	486	484	484	496	488	7.946	2.54	1.573	49.7
35	486	484	481	496	487	7.725	2.47	1.585	49.3
40	486	484	481	496	487	3.125	1.00	1.765	43.5
41	484	484	484	496	487	0	0	1.316	57.9
50	484	484	484	496	487	0	0	1.313	58.0
51	484	484	484	496	487	3.059	0.98	2.080	35.4
56	484	484	484	496	487	0	0	1.305	58.2
57	484	484	484	496	487	3.059	0.98	2.016	35.5
58	484	484	484	496	487	0	0	1.339	57.2
59	484	484	484	496	487	3.059	0.98	2 050	34.4
60	484	484	484	496	487	0	0	1.330	57.4

*) This Table is reproduced from the paper of I. TOYOSHIMA and J. HORIUTI (this Journal, **6**, 149 (1958)).

**) The t_1, t_2, t_3 and t_4 are temperatures measured at different positions of the catalyst bed packed in a vertical quartz cylinder, gas mixture being passed through it from the top to the bottom; t_1, t_2 and t_3 are readings of thermojunctions on the axis of the bed, respectively at the top, middle and bottom, and t_4 is that on the wall at the middle.

TABLE 1(b). Hysteresis of ammonia decomposition

Inflow rate N_A of NH_3: 4.465×10^{-1} mol min^{-1} = 100 cc NTP min^{-1}

No. of runs	Temperature※) (°C)					Inflow rate N_H of H_2 mol $min^{-1}\times10^3$	$\frac{N_H}{N_A}$	Outflow rate N_A of NH_3 mol $min^{-1}\times10^3$	Percent decomposition of NH_3 $R\equiv100\frac{N_A-N'_A}{N_A}$
	t_1	t_2	t_3	t_4	ave.				
1	—	430	435	438	434	17.73	3.97	1.432	67.9
2	—	430	435	440	435	13.53	3.03	1.272	71.5
3	—	430	435	440	435	8.930	2.00	1.103	75.3
4	—	430	435	440	435	4.600	1.03	0.827	83.7
5	—	429	435	439	434	2.247	0.50	1.004	77.5
6	—	429	435	440	435	1.626	0.36	0.951	78.7
7	—	431	434	440	435	0.893	0.20	1.116	75.0
8	—	430	435	439	435	0.411	0.09	1.312	70.6
9	—	430	435	438	434	0	0	1.326	70.3
10	—	430	435	438	434	0.848	0.19	1.500	66.4
11	—	430	435	438	434	2.241	0.50	1.848	58.6
12	—	430	435	438	434	6.700	0.15	2.116	52.6
13	—	430	434	440	435	0	0	1.205	73.0
14	—	432	435	438	435	4.556	1.02	2.085	53.3
15	—	430	435	438	434	8.930	2.00	1.936	56.6
16	—	430	435	440	435	1.102	2.47	1.307	70.7
17	—	430	435	440	435	13.31	2.98	1.388	68.9
18	—	430	435	440	435	17.58	3.94	1.437	67.8
19	—	432	435	440	436	17.78	3.98	1.349	69.8
20	—	432	435	440	436	15.40	3.45	1.254	71.9

21	—	430	435	440	435	17.78	3.98	1.349	69.8
22	—	430	435	440	435	15.40	3.45	1.316	70.5
23	—	430	435	440	435	11.16	2.50	1.156	74.1
24	—	430	435	440	435	7.190	1.61	0.924	79.3
25	—	428	435	440	434	3.483	0.78	0.839	81.2
26	—	431	435	441	436	0.848	0.19	1.267	71.6
27	—	429	435	438	434	0	0	1.352	69.7
28	—	430	435	438	434	2.250	0.50	1.861	58.3
29	—	429	437	437	434	4.465	1.00	2.231	50.0
30	—	430	437	437	435	4.465	1.00	2.178	51.2

*) *Cf.* footnote **) to Table 1(a).

TABLE 1(c). Hysteresis of ammonia decomposition

Inflow rate N_A of NH_3: 4.465×10^{-3} mol min^{-1} = 100 cc NTP min^{-1}

No. of runs	Temperature*) (°C)					Inflow rate N_H of H_2 mol $min^{-1}\times10^3$	$\frac{N_H}{N_A}$	Outflow rate N_A of NH_3 mol $min^{-1}\times10^3$	Percent decomposition of NH_3 $R\equiv100\,\frac{N_A-N'_A}{N_A}$
	t_1	t_2	t_3	t_4	ave.				
1	425	427	440	440	433	17.87	4.00	1.182	73.5
2	425	427	440	440	433	13.53	3.03	0.924	79.3
3	425	427	440	440	433	10.49	2.35	0.670	85.0
4	425	427	440	440	433	4.598	1.03	0.513	88.5
	total ave. 433								

*) *Cf.* footnote **) to Table 1(a).

the upper one. These catalysts are designated by Catalyst–I, –II and –III respectively in what follows.

§ 2. Experimental procedures

Specimens. Catalyst–I was sampled as follows from the catalyst used for the experiment of Fig. 1 (a) with details shown in Table 1 (a). After completion of the last run shown in the Table, the catalyst was cooled down to around 200°C by removing the electric furnance quickly, allowing at the same time the gas mixture to flow constantly over the catalyst. The gas mixture was then replaced with nitrogen and the catalyst was cooled down to room temperature. The catalyst were then dropped layer by layer, each across the line of flow in the bed, separately into benzene-filled flasks in nitrogen atmosphere to secure catalyst's surface from oxidation. The layers thus separated were numbered 1, 2,…… in their order along the line of flow.

Catalyst–II was prepared by a separate series of experiments, similar to that of Fig. 1 (a), with the result shown in Table 1 (b) and Fig. 1 (b). The catalyst was much more active in this case, so that the temperature of the catalyst had to be lowered and the flow rate to be increased in order to reduce R to a value reasonably below 100 hence practically dependent on the flow rate. The inflow rate of ammonia was thus fixed at 100 cc NTP min^{-1} and the temperature of the catalyst at 435°C. The hysteresis was followed as shown in Fig. 1 (b) somewhat different from Fig. 1 (a), and finally interrupted at the point II in Fig. 1 (b) to sample the catalyst similarly as in the case of Catalyst–I.

Catalyst–III was prepared similarly at fixed inflow rate 100 cc NTP min^{-1} of ammonia and at the temperature 433°C of the catalyst without tracing the hysteresis completely but interrupting it at point III in Fig. 1 (c) on the curve of R increasing with decrease of N_H/N_A.

X-ray examination. The specimens for x-ray examination were prepared from Catalyst–I, –II and –III by securing them from oxidation as follows. A part of the catalyst stored in the benzene-filled flask was transferred into 1% solution of collodion in alcohol-ether and pulverized, except in the case of Catalyst–I, which was sufficiently pulverized by the repeated hysteresis cycles, in the agate mortar as it was wet with the collodion solution, and part of the pulverized catalyst was taken into a glass capillary and dried there. DEBYE-SCHERRER photographs of the thin rods thus prepared were taken with filtered Fe-K_α radiation to identify the constituent phases of the catalyst. The rest of the pulverized catalyst was dried in the agate mortar to prepare the sample for accurate measurements of lattice parameter with counter-diffractometer (Norelco). The catalyst powder thus dried was pressed into sample-holder of the diffrac-

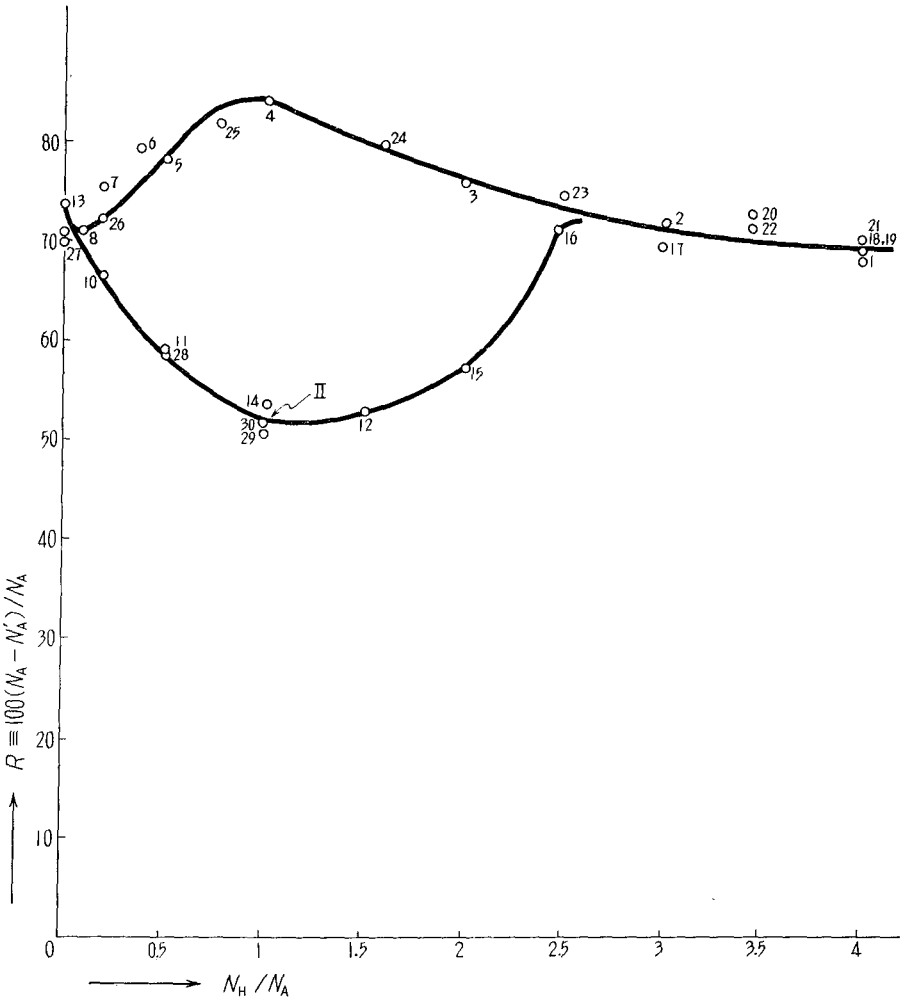

Fig. 1 (b). Hysteresis of percent R of ammonia decomposition. 435°C, $N_A = 100$ cc NTP min^{-1}.

tometer at approximately constant pressure. The holder was rotated upon the axis perpendicular to the diffractometer axis and normal to the face of the holder during measurement of diffraction pattern. The patterns were obtained by means of strip-chart recording method, using filtered Co-K_α radiation. The voltage input to the x-ray tube was maintained at 35 kv and the tube current at 7 mA throughout all the measurements by means of electronic stabilizer.

Electron diffraction. The surfaces of Catalyst-II and -III were examined

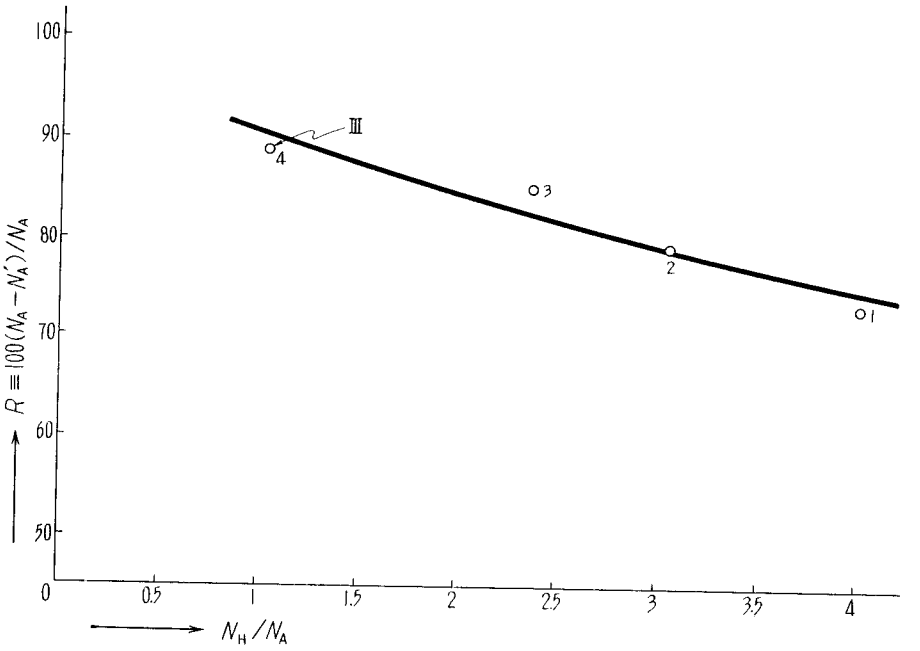

Fig. 1 (c). Hysteresis of percent R of ammonia decomposition. 433°C, $N_A = 100$ cc NTP min^{-1}.

by electron diffraction, before the surface replicas were prepared for electron microscopy. The catalyst grain with relatively flat surface was mounted on sample-holder, as it was wet with benzene for storage, placed in the diffraction apparatus and then dried in vacuo. Electron beams were accelerated at from 35 to 40 kv, the values of $L\lambda$ (camera length × wave length) being determined by reference to that of Au-foil.

Electron microscopy. Since the reduced catalysts are highly porous and reactive, it is quite difficult to replicate the details of the surface. Surface replicas of the present catalyst were prepared by two-step process. The first replica was ethylcellulose deposited over the catalyst's surface from the solution in trichloroethylene and the second one was thin film of evaporated carbon. Although the pre-shadowed carbon replica excels others in resolving power, it was impracticable for this catalyst because of fragmentation of the replica caused by gas-evolution associated with dissolution of the catalyst in etchant. The latter preparative technique of replica was, however, adequately applied to the specimen of iron single crystal inserted in the bed of Catalyst-II.

These techniques were practised as below:

Two-step process. The catalyst wet with benzene for storage was dried in vacuo and then the surface of the catalyst was coated with 2% solution of ethylcellulose in trichloroethylene to make the first replica. The first replica was now loosened by razor edge and peeled off from the surface, and then shadow-casted with chromium metal. The second replica was prepared by usual technique of carbon replica. Residual tiny particles of the catalyst, with which the replica was stained, were dissolved in dilute hydrochloric acid. This preparative technique did not give replicas with high resolving power, but reproducible results.

Pre-shadowed carbon replica. The surface of the specimen of iron single crystal was first shadow-casted with Cr and then carbon was evaporated on the shadowed surface. The carbon film thus formed was separated, after being scored to give about 1 mm square, from the surface by dissolving the surface layer of the specimen in usual etchant.

§ 3. Constituent phases of catalyst

The constituent phases of the catalysts were examined by x-ray and electron diffraction. Table 2 shows the constituent phases thus identified.

Catalyst-I or -III is found, as shown in the second column of the Table, to be composed respectively of γ'- or α-phase exclusively except at the inlet of the catalyst bed. X-ray patterns from the layers near the inlet, *i. e.* Catalyst-I-1 and -2, show a very small amount of ε-phase coexisting with the main phase of γ' and Catalyst-III-1 does similarly a small amount of γ'-phase coexistent with main α-phase. Catalyst-II on the other hand is composed solely of γ'-phase at the inlet of the bed, α-phase increasing towards the outlet and solely of α-phase at the outlet.

The third column shows the constituent phases of the surfaces of Catalyst-II and -III identified by electron diffraction. They are almost the same as those in the interior in case of Catalyst-III, but somewhat different in case of Catalyst-II, both α- and γ'-phases existing comparably in amounts on the surface at the inlet of the bed. This aspect is ascribable to the reduction of γ'-phase on the surface in course of cooling the bed down to 200°C in the flow of gas mixture. The percent of ammonia in gas phase in equilibrium of the reaction $4Fe + NH_3 = Fe_4N + 3/2\ H_2$ is extrapolated at 59.6% for 300°C from the equilibrium constant $(P_{H_2})^3/(P_{NH_3})^2$ observed by EMMETT *et al.*[3]. Since the percent of ammonia in the equilibrium is still greater at lower temperature, the $N_H/N_A = 1$ gas mixture should reduce the catalyst's surface to α-phase at temperature below 300°C as mentioned above in accordance with the theory of the hysteresis advanced by TOYOSHIMA and HORIUTI[1].

The electron diffraction patterns from surfaces of the specimens of iron single crystal II-S-1, -2 and -3 inserted in the bed of Catalyst-II show that the constituent phases of the surface vary similarly to those of the catalyst

TABLE 2 Constituent phases and their lattice parameters

Specimen	Phase		Lattice parameter (Å)	
	X-ray diffraction	Electron diffraction	γ'-phase	α-phase
Catalyst-I				
1	γ' with faint ε	—	3.7986	—
2	γ' with faint ε	—	3.7987	—
3	γ' only	—	3.7985	—
4	γ' only	—	3.7985	—
5	γ' only	—	3.7985	—
6	γ' only	—	3.7983	—
7	γ' only	—	3.7982	—
8	γ' only	—	3.7983	—
9	γ' only	—	3.7982	—
Catalyst-II				
S-1	α with very faint γ'	γ' and α	—	—
1	γ' only	γ' and α	3.7982	—
2	γ' with faint α	γ' and α	3.7980	—
3	γ' and α	γ' and α	3.7980	2.8667
S-2	α with very faint γ'	α with faint γ'	—	—
4	γ' and α	α with faint γ'	3.7980	2.8666
5	γ' and α	α only	3.7978	2.8665
6	α only	α only	—	2.8656
S-3	α only	α only	—	—
Catalyst-III				
1	α with faint γ'	α with faint γ'	—	2.8655
2	α only	α only	—	2.8661
3	α only	α only	—	2.8656
4	α only	α only	—	2.8661
5	α only	α only	—	2.8657
6	α only	α only	—	2.8657
7	α only	α only	—	2.8655

along the line of flow, whereas the x-ray patterns indicate that the interior of the specimen consists almost constantly of α-phase. These specimens of iron single crystal were now immersed in usual etchant to remove the surface layer and reexamined by electron diffraction; the diffraction patterns were quite the same N-patterns with KIKUCHI lines as observed before the treatment with the

gas mixture. These results show that the nitrification and reduction of the catalyst are only superficial under the present experimental conditions.

§ 4. Lattice parameters of the γ'- and α-phases

Lattice parameters of the γ'- and α-phases were determined for each layers of the catalyst bed by comparing some reflections of x-ray from the phases with those from internal reference. The lattice parameters thus determined are shown in the fourth and fifth columns of Table 2. Any of them is the mean of two values *e. g.* 3.7988 Å and 3.7984 Å for Catalyst-I-1, respectively determined from the comparison of (200)-reflection of the γ'-phase with (220)-reflection of silicone metal*) used as the internal reference and of (220)-reflection of the former with (400)-reflection of the latter. In the case of the α-phase, (110)- and (211)-reflections were compared respectively with (220)- and (422)-reflections of sodium chloride*) with the results, *e. g.* 2.8651 Å and 2.8659 Å respectively for Catalyst-III-1.

Accuracy of such determination of lattice parameter may depend practically solely on that of determination of angular separation between the reflections to be compared, hence on the accuracy of determination of the position of reflection peak, provided that both the reflections are near each other. The accuracy in the case of Catalyst-I is in consequence higher than those in the other cases because of the sufficiently resolved K_α-doublet ascribable to the well-grown crystallites resulting from the hysteresis cycles repeated so many a time. Mean error of a single observation of the lattice parameter was 0.0002 Å in the case of Catalyst-I, whereas 0.0005 Å in the other cases. It follows from the observation of the above accuracy that the lattice parameter of γ'-phase of Catalyst-I decreases slightly along the line of gas flow, whereas that both of γ'- and α-phases of Catalyst-II and -III remain respectively constant along the line of flow within the experimental errors.

The lattice parameter of the γ'-phase thus found is slightly larger than that reported by HÄGG[6] and JACK[7], who obtained 3.795 Å at the maximum content of nitrogen, *i. e.* 6.1%; that of the α-phase of Catalyst-II or -III found at 2.8666 or 2.8657 Å in the present work is in agreement within the experimental error with the value of α-iron, 2.86624 Å reported by JETTE and FOOTE[8].

*) The values of 2 θ of silicon metal and sodium chloride used as internal references have been quoted from "The TECHNICAL REPORT of Philips Laboratories, No. 68, (1953)", where the lattice parameters of Si and NaCl at 21°C are given as 5.43062 Å and 5.63937 Å respectively.

§ 5. Nitrogen content in catalyst

The constituent phases of the catalyst vary along the line of gas flow as mentioned in § 3. Since the ε-phase coexists with the γ'-phase just about the inlet of the catalyst bed in the case of Catalyst–I, nitrogen content of the γ'-phase may decrease along the line of flow in accordance with the phase diagram[9]. This inference is consistent with the decrease of the lattice parameter of the γ'-phase of Catalyst–I along the line of flow as shown in Table 2, which is accompanied by decrease of the nitrogen content as observed by EISENHUT and KAUPP[10] and PARANJPE *et al.*[11]. The same may be the case with the nitrogen content of the α-phase of Catalyst–III, where γ'-phase coexists with the α-phase just at the inlet of the catalysts bed but disappears in the subsequent layers, as shown in Table 2. The nitrogen content of the γ'- and α-phases of Catalyst–II may also decrease along the line of flow except at the middle portion of the bed where they coexist.

The lattice parameter of γ'-phase, according to PARANJPE *et al.*, increases from 3.791 Å at 5.29% nitrogen content to 3.801 Å at 5.71% nitrogen content. Assuming that the lattice parameter increases linearly with the nitrogen content, the observed value of lattice parameter 3.7987 Å or 3.7978 Å of the γ'-phase of Catalyst–I–2 or Catalyst–II–5, where the γ'-phase coexists respectively with ε-phase or α-phase, corresponds respectively to 5.62 or 5.58% nitrogen content. These compositions represent those both at the extremities of γ'-phase on the phase diagram, which could not be obscured by some inaccuracies in the separation of layers*), inasmuch as the lattice parameter of the γ'-phase is constant within the experimental error over a few layers both at the extremities. It follows in consequence that the γ'-phase observed in the present work is limited within very narrow range of nitrogen content as compared with the case of PARANJPE *et al.* and other workers[3,10,12], where pure iron powders were used as material. Such a difference in nitrogen content might be attributed to an effect of the promoter comprized in the catalyst.

BURNS[13] showed, on the other hand, that the lattice parameter of α-phase is 2.8663, 2.8668 and 2.8685 Å respectively at 0.004, 0.015 and 0.10% nitrogen content. The nitrogen content of α-phase of Catalyst–II–3, where it coexists with γ'-phase, is interpolated at 0.013% for the observed lattice parameter 2.8667 Å from the above result of BURNS. This value of nitrogen content at the coexistence of α-phase with γ'-phase is smaller than that interpolated at 0.031% from the result of DIJKSTRA[14] on solubility of nitrogen in α-iron for

*) *cf.* § 2.

the present reaction temperature 435°C. Admitted that this difference is outside the experimental errors, it is concluded that the nitrogen content of α-phase is reduced by addition of the promoter.

§ 6. Electron microscopy

Catalyst–III. There is a wide variety of the surface features. Common features to all the layers are "pore" and "crack" structures as seen in micrograph of Fig. 2. This "pore" structure resembles that observed by McCARTNEY and ANDERSON[15] with fused iron catalyst promoted with MgO and K_2O. The "pore" size has been estimated from the micrograph at 300 to 400 Å. Another micrograph, Fig. 3, obtained with the same specimen shows aggregates of catalyst particles as well as their replicas.

The particles were further examined by transferring them to carbon film*) from the first replica stained with them. Fig. 4 shows the particles thus retained on the carbon film, the size of which is estimated at several hundreds angstroms. This size is approximately in agreement with that of crystallites of the catalyst as observed by x-ray[16], which suggested that each particle is an individual crystallite, hence that the catalyst is composed of the particles and the "pore" is nothing but the intergranular void. The "cracks" are attributed to the intersections of the surface with (111)-planes of unreduced catalyst.

Catalyst–II. The "pore" and "crack" structures of the surface of this catalyst are not much different from those of Catalyst–III, as shown in Figs. 5 and 6, except that they are rather indistinct in this case. Fig. 7 shows a pre-shadowed carbon replica of the surface of the catalyst powder retained on surface of the specimen of iron single crystal. This does not show the "pore" structure, but only granular one. With due regard to the higher resolving power of this replica than that of the two-step process, this result confirms the conclusion that the "pore" observed by the two-step process is but the intergranular void. No remarkable changes of the surface features of the catalyst is observable along the line of gas flow similarly as in the case of Catalyst–III.

*) The particles of the catalyst were tranferred to carbon film as follows: an optical deck-glass was first covered with gelatine film from aqueous solution and was then further covered with 10% solution of collodion in alcohol-ether. Just before the collodion was dried, the first replica stained with residual particles was pressed against the deck-glass coated doubly as above. After the collodion was dried, the first replica was detouched from the deck-glass. Carbon film was now deposited by evaporation on the collodion film on which the particles were now retained and the collodion film was then dissolved in alcohol-ether to leave the particles on the carbon film.

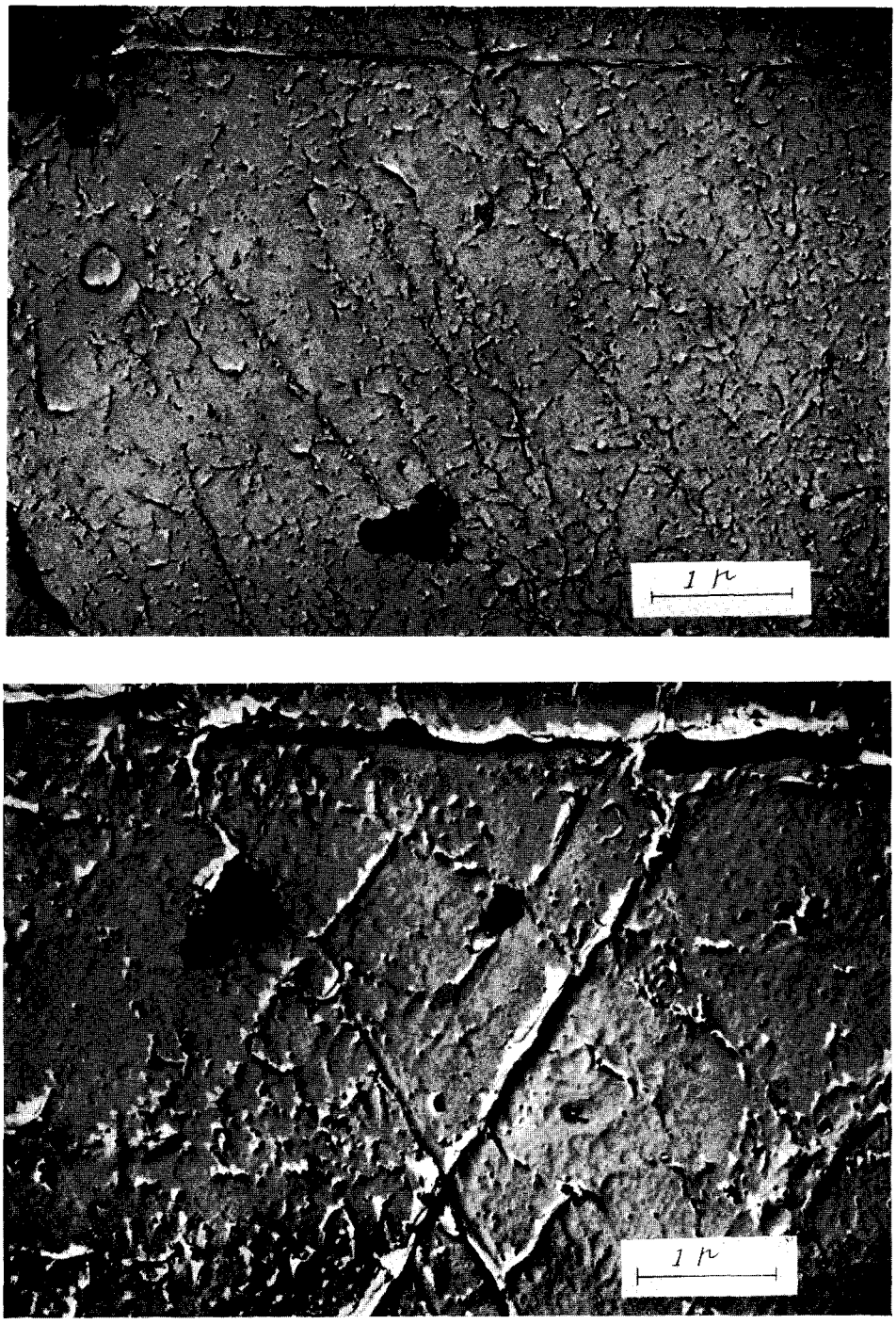

Fig. 2. The "pore" and "crack" structures of Catalyst-III. ×24,000

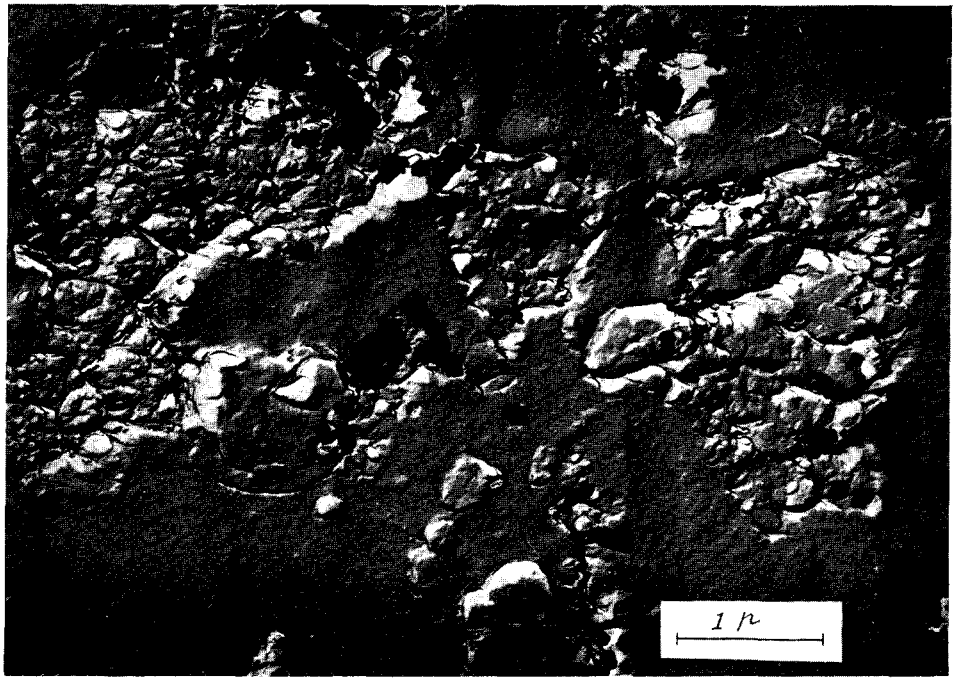

Fig. 3. Replica of aggregates of the catalyst particles, showing some residual particles ×24,000

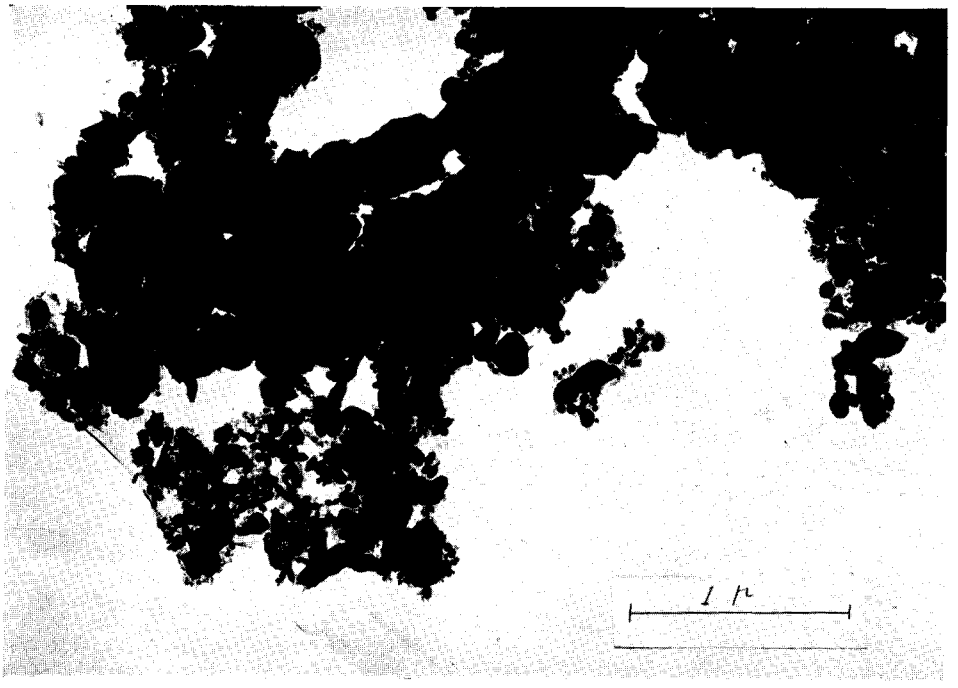

Fig. 4. The catalyst particles transferred onto carbon film. ×36,000

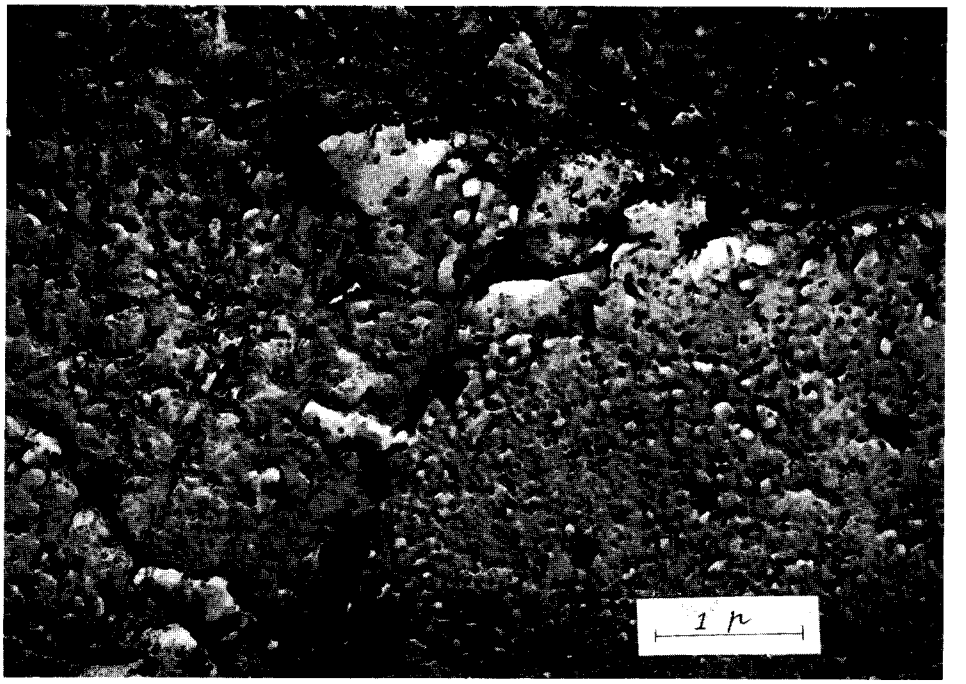

Fig. 5. The "pore" structure of Catalyst-II. ×24,000

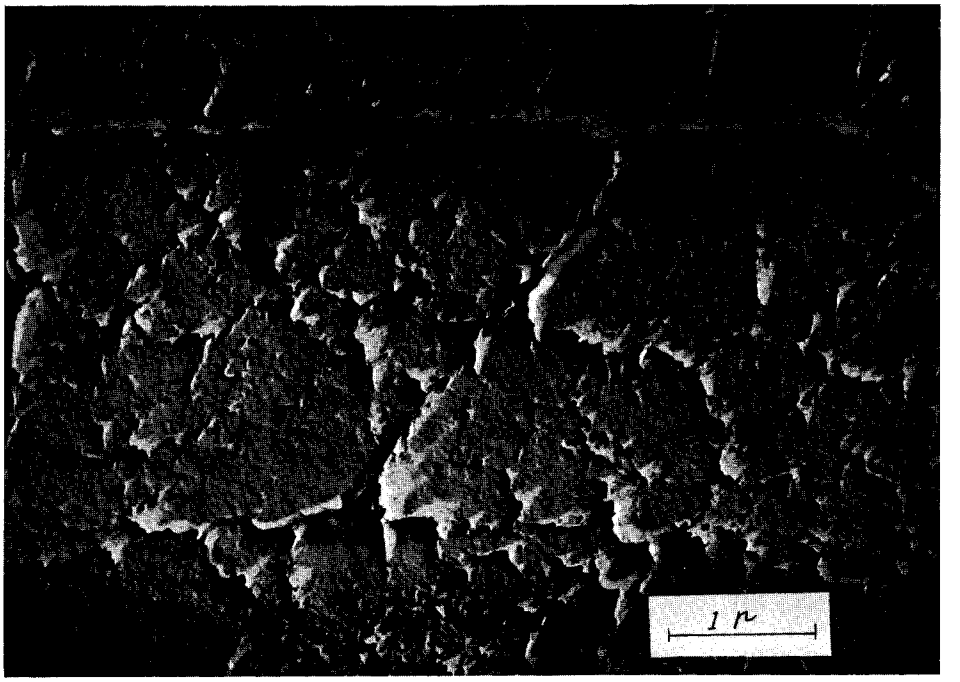

Fig. 6. The "crack" structure of Catalyst-II. ×24,000

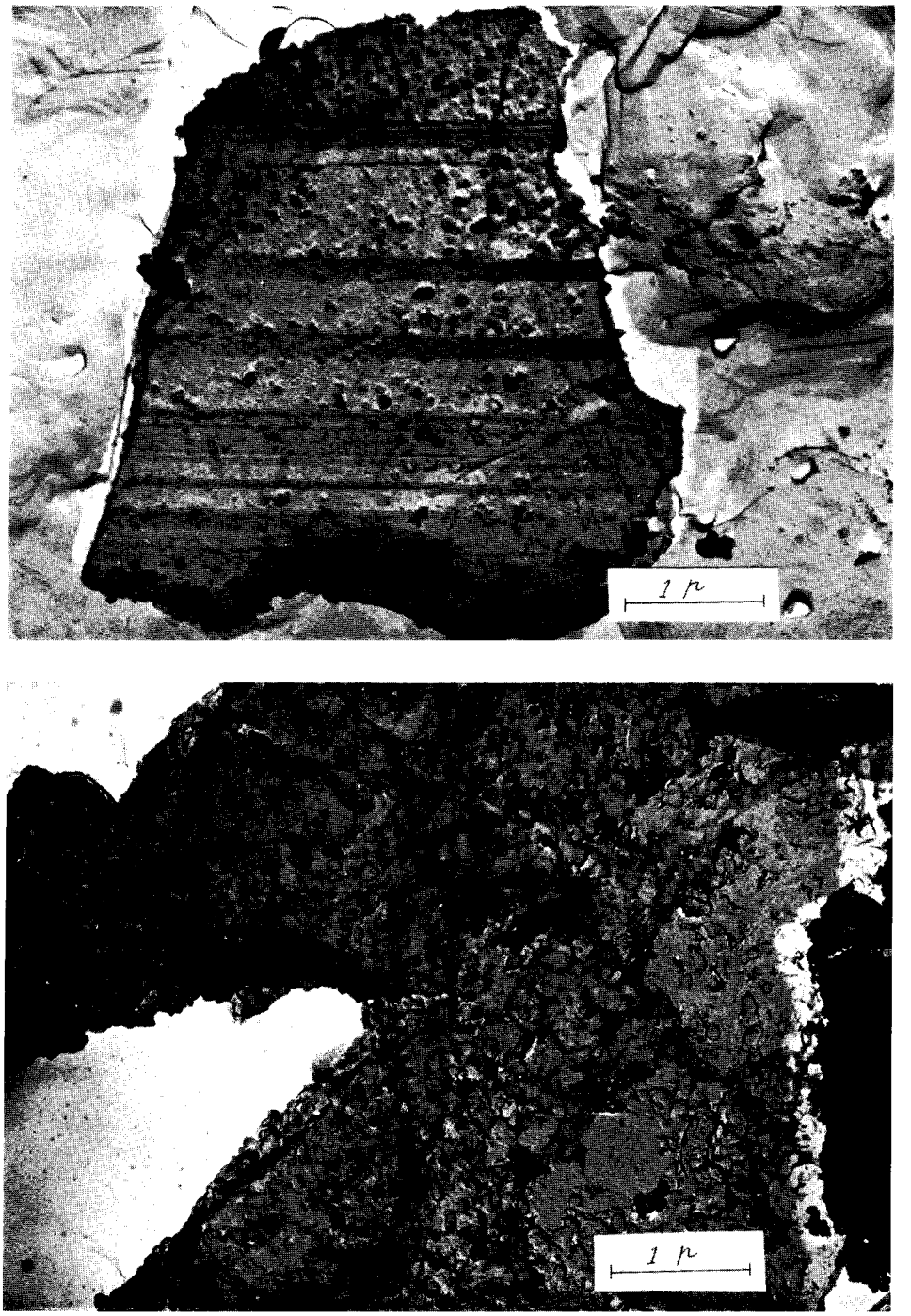

Fig. 7. Pre-shadowed carbon replica of Catalyst-II retained on the specimen of iron single crystal. ×24,000

The surface features of the specimen of iron single crystal do vary, however, remarkably along the line of flow, as shown in Figs. 8, 9 and 10. It is concluded from these electron micrographs with reference to the results of electron diffraction studies on the surfaces that the major part of the surface of the specimen at the inlet is covered with well-developed crystallites of γ'-phase and minor part with tiny particles of α-phase produced presumably by reduction during the cooling of the catalyst's bed*) (Fig. 8), whereas the surface at the middle of the catalyst bed is almost covered with the tiny particles of α-phase as shown in Fig. 9, which are in turn replaced towards the outlet completely by fine growth-steps and a few projections on the surface as seen in Fig. 10. Such a difference of the surface features between the catalyst and the iron single crystal may be due to the promoter in the catalyst inhibiting surface migration of iron atoms.

*) *cf.* § 2.

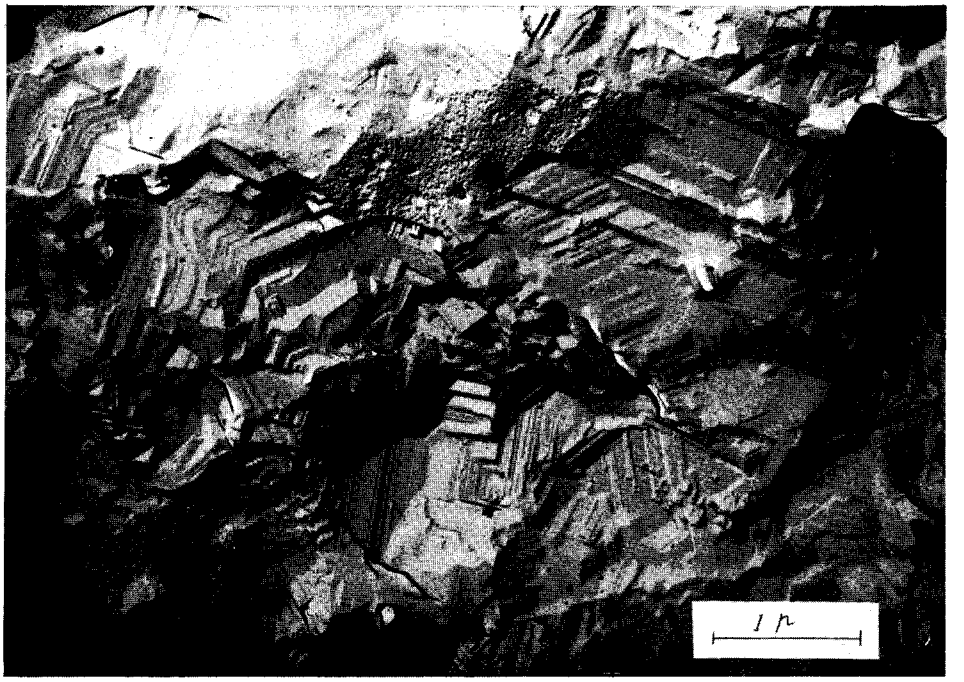

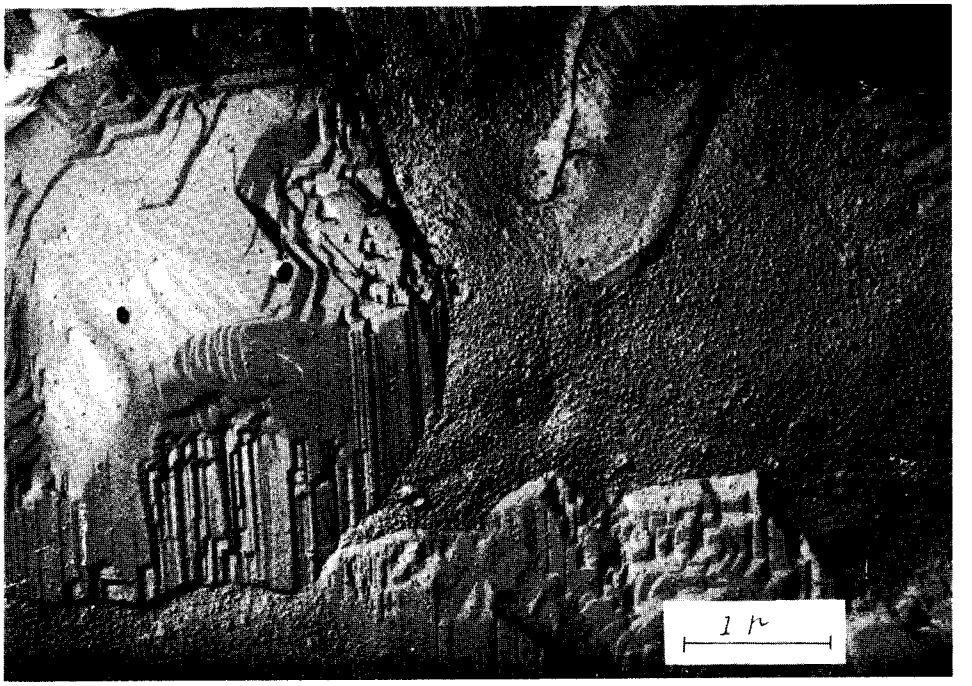

Fig. 8. Pre-shadowed carbon replica of iron single crystal, at the inlet of the bed. ×24,000.

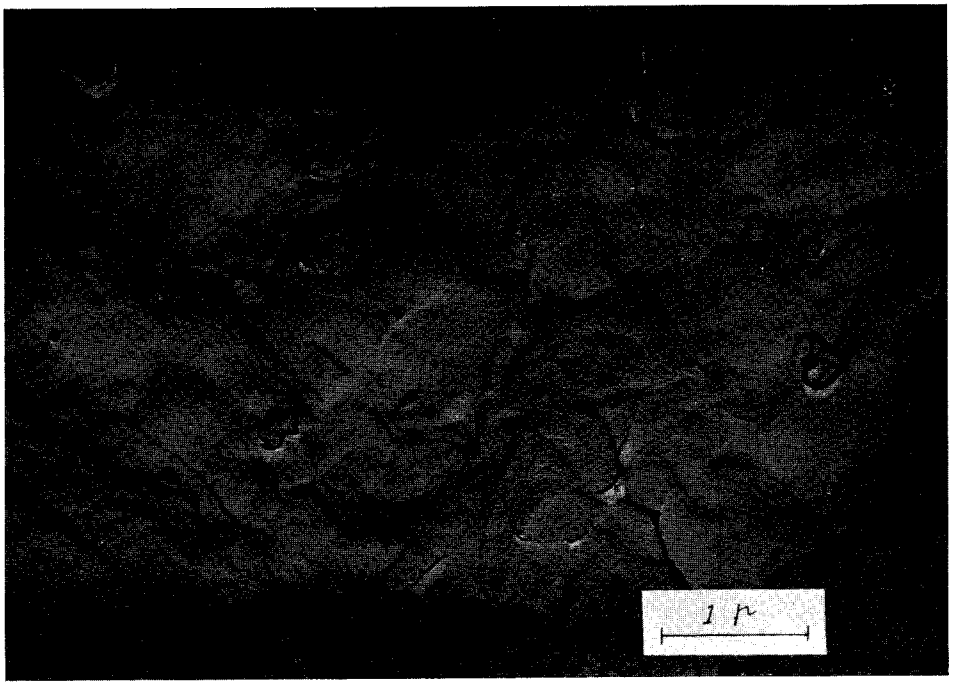

Fig. 9. Ditto, at the middle of the bed. ×24,000

§ 7. Conclusion

TOYOSHIMA and HORIUTI have concluded[2] by analysing the experimental results of catalyzed decomposition of ammonia inclusive of the hysteresis in question that the decomposition proceeds through the sequence of steps

$$NH_3 \longrightarrow NH_2\,(a) + H\,(a)$$
$$NH_2\,(a) \longrightarrow NH\,(a) + H\,(a)$$
$$NH\,(a) \longrightarrow N\,(F) + H\,(a) \qquad (1)$$
$$N\,(F) \longrightarrow N\,(a) \qquad (2)$$
$$2N\,(a) \longrightarrow N_2 \qquad (3)$$

and

$$2H\,(a) \longrightarrow H_2$$

and that the decomposition rate is governed by the step (1) on α-phase and by the step (2) or (3) on γ'-phase, where N (F) is nitrogen atom absorbed in the catalyst.

According to this mechanism, on which basis the hysteresis was explained[1],

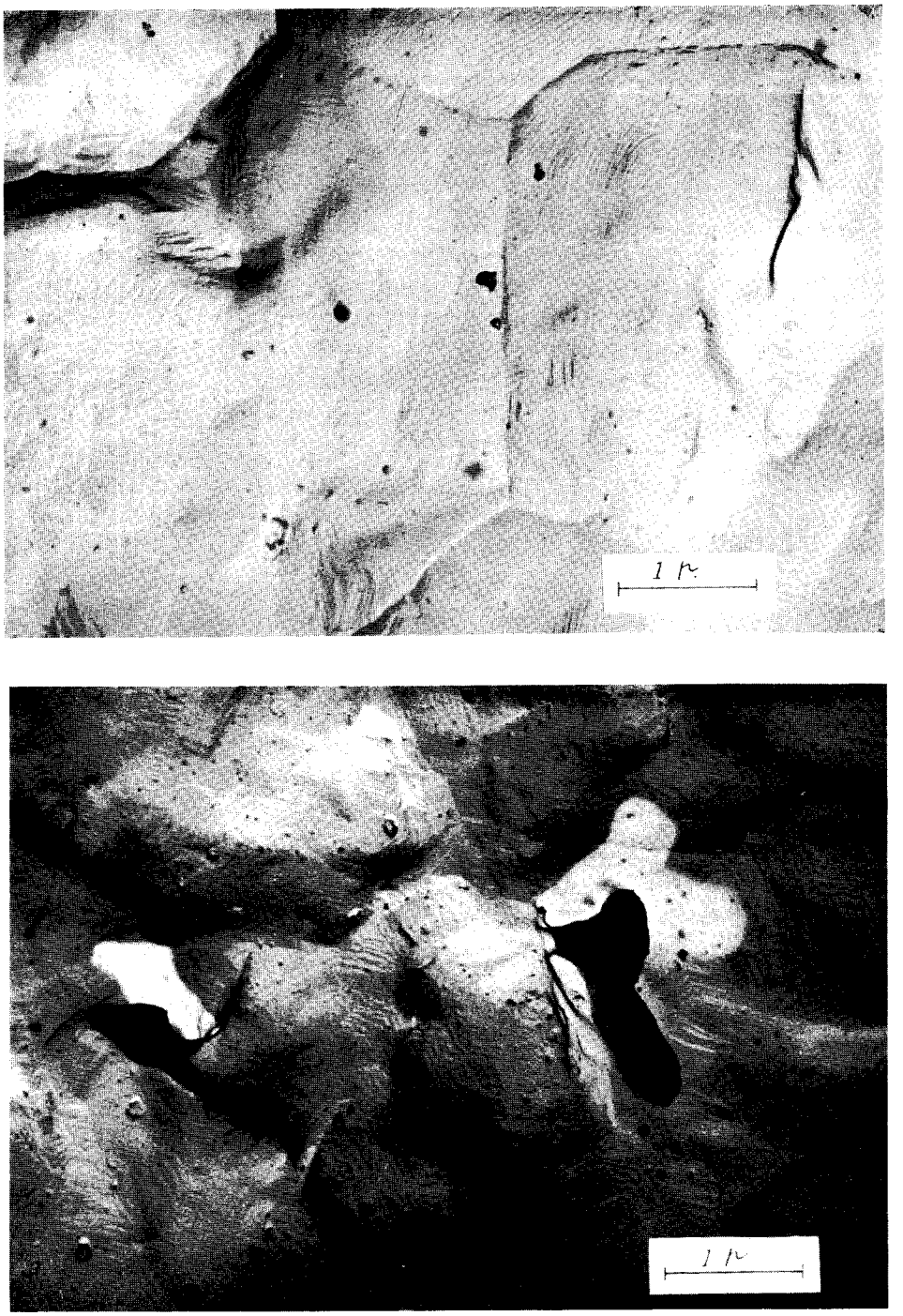

Fig. 10. Ditto, at the outlet of the bed. ×24,000

the catalyst's surface remains stably in the state of α-phase, even when N_H/N_A at the steady decomposition is decreased below its value $(N_H/N_A)_0$ in equilibrium of the reaction $4Fe + NH_3 = Fe_4N + 3/2\ H_2$ by a certain amount, beyond which the decrease of N_H/N_A results in nitrification of α-phase to γ'-phase first at the inlet of the bed and progressively towards the outlet. As N_H/N_A at the steady decomposition is increased on the other hand from zero, the catalyst's surface remains stably at the inlet in the state of γ'-phase so long as N_H/N_A does not exceed $(N_H/N_A)_0$, inasmuch as N (F) is then in equilibrium with hydrogen and ammonia according to the mechanism ; but since the ratio of the flow rate of hydrogen to that of ammonia increases with progress of decomposition of ammonia along the line of flow in the bed, the catalyst is reduced first at the outlet from γ'-phase to α-phase and progressively towards the inlet with increase of N_H/N_A.

The above conclusion arrived at by TOYOSHIMA and HORIUTI[1] about the constituent phases of the catalyst are satisfactorily confirmed by the results shown in Table 2, with which Catalyst–III and –II were examined layer by layer along the line of gas flow in the catalyst bed.

Summary

1. The catalysts were examined by x-ray, electron diffraction and electron microscopy at three typical points on the hysteresis loop of the rate of steady decomposition of ammonia, *i. e.* the steady rate of decomposition of ammonia on a bed of doubly promoted synthetic catalyst kept at around 450°C was plotted against N_H/N_A of ammonia-hydrogen mixture at 1 atm. total pressure, where N_A is the inflow rate of ammonia fixed at 70 or 100 cc NTP min^{-1} and N_H is that of hydrogen kept constant until the steady decomposition is attained and thus stepwise decreased from 4 N_A to zero and then similarly increased. The catalyst examined were those at the states represented by three points on the hysteresis loop, *i. e.* that on the upper curve (Catalyst–III), that on the lower one (Catalyst–II) and that at the point $N_H/N_A = 0$ (Catalyst–I).

2. X-ray examination showed that Catalyst–I or –III consisted exclusively of γ'-phase or α-phase respectively except at the inlet of the catalyst bed, where a small amount of ε-phase or γ'-phase coexisted with the respective main phases. Catalyst–II, on the other hand, was composed solely of γ'-phase or α-phase at the inlet or the outlet of the bed, both the phases coexisting at the middle. Nitrogen content of the γ'-phase or α-phase decreased along the line of flow as inferred from the observations of the lattice parameter and the coexistent phases. These results and the relevant inference are consistent with the conclusion drawn by TOYOSHIMA and HORIUTI[1].

3. Electron micrographs of the surfaces of Catalyst–II and –III exhibited "pore" and "crack" structures, wich were shown ascribable to intergranular voids and to the intersections of the surface with cleavages at (111)-planes of unreduced catalyst respectively.

4. The surface texture of catalyst mentioned in § 6. remains almost unchanged along the line of flow, whereas that of specimens of iron single crystal inserted in the bed of Catalyst–II varied remarkably; the surface was covered with the well-developed crystallites of γ'-phase at the inlet, with the tiny particles of α-phase at the middle and with fine growth-steps at the outlet. This difference between the catalyst and the specimen of iron single crystal was plausibly attributed to inhibition of sintering by promoter in the catalyst.

Acknowledgments

The authors wish to thank Professor J. HORIUTI, the director of this Institute, for encouragement and helpful discussions throughout the course of the work and Dr. S. HARIYA for the use of "Norelco".

Reference

1) I. TOYOSHIMA and J. HORIUTI, This Jouanal **6**, 146 (1958).
2) J. HORIUTI and I. TOYOSHIMA, *ibid.* **5**, 120 (1957).
J. HORIUTI and I. TOYOSHIMA, *ibid.* **6**, 68 (1958).
3) P. H. EMMETT, S. B. HENDRICKS and S. BRUNAUER, J. Am. Chem. Soc., **52**, 1456 (1930).
S. BRUNAUER, M. E. JEFFERSON, P. H. EMMETT and S. B. HENDRICKS, *ibid*, **53**, 1778 (1931).
4) M. TEMKIN and V. PYZHEV, Acta Physicochim. U.S.S.R., **17**, 324 (1940).
K. S. LOVE and P. H. EMMETT, J. Am. Chem. Soc., **63**, 3297 (1941).
5) S. ENOMOTO and J. HORIUTI, This Journal, **2**, 87 (1952).
S. ENOMOTO, J. HORIUTI and H. KOBAYASHI, *ibid.* **3**, 155 (1955),
6) G. HÄGG, Nova, Acta Soc. Sci. Upsal, **IV 7**, 1 (1929).
7) K. H. JACK, Proc. Royal Soc., **A 195**, 34 (1948).
8) E. R. JETTE and F. FOOTE, J. Chem. Phys., **3**, 605 (1935).
9) M. HANSEN, *Constitution of Binary Alloys*, 2nd ed., pp. 670, McGaw-Hill Book Co. Inc., New York, (1958).
10) O. EISENHUT and E. KAUPP, Z. Elektrochem., **36**, 392 (1930).
11) V. G. PARANJPE, Morris COHEN, M. B. BEVER and C. F. FLOE, Transaction AIME., **188**, 161 (1950).
12) K. H. JACK, Proc. Royal Soc., **A 208**, 200 (1951).
13) J. L. BURNS, Transaction AIME., **113**, 239 (1934).
14) L. J. DIJKSTRA *ibid.* **185**, 252 (1949).
15) J. T. MCCARTNEY and R. B. ANDERSON, J. Appl. Phys., **22**, 1441 (1951).
16) T. MATSUI and I. TOYOSHIMA, This Journal, to be appeared in the next publication.